Diffusion of water vapour in cellulose acetate: 2. Permeation and integral sorption kinetics

P. P. Roussis
Physical Chemistry Laboratory, 'Demokritos' Nuclear Research Center, Chemistry Department, Aghia Paraskevi Attikis, Athens, Greece
(*Received* 7 *July* 1980; *revised* 15 *October* 1980)

A series of permeation and integral sorption kinetic experiments were performed under both absorption and desorption conditions on membranes of cellulose acetate prepared by the same methods and conditions as before[1]. Alternative methods of data treatment are presented. The slow approach to steady state as well as analysis of time lag data suggest that the limiting value of the thermodynamic permeability coefficient is approached at a slow rate. In view of a comparable time-variability already observed in the solubility coefficient[1], these results indicate that the mobility of penetrant molecules does not decrease with time; hence they imply that the effect of partial immobilisation of the water molecules in clusters is offset by polymer plastisization caused by the penetrant. The diffusion coefficient D is shown to increase with concentration in all cases, thus confirming the conclusions based on differential sorption data. D measured in absorption is, at any concentration, lower than in desorption, but in desorption it shows satisfactory agreement between the two limbs of the equilibrium isotherm.

INTRODUCTION

In part 1[1] (which dealt with differential sorption kinetics at various vapour activities a and membrane thickness l) we concluded that two rate-controlling relaxation processes accompanying diffusion could be distinguished. The first of these, which occurs during the early stages of absorption, is simply a reorganization of the already existing free volume as well as a minor expansion of the polymer which is necessary for the reception of a certain concentration C_m of monomeric water vapour[2]. The second, involves a more extensive polymer swelling and hence requires more drastic rearrangement of its network, so that more penetrant can be accommodated in the form of clusters[1-5] (associated water molecules) to a concentration C_a. This led to the conclusion that the total vapour concentration $C=C_m+C_a$ in the membrane, or the solubility coefficient $S=C/a$ are increasing functions of time t; i.e. $S=S(a,t)$, $C=C(a,t)$. However, distinction of the time effects on S and on the thermodynamic permeability P_T, as defined in the following forms of the diffusion equation[6] (in which X is the axis of diffusion and D_T the thermodynamic diffusion coefficient):

$$\frac{\partial C}{\partial t}=\frac{\partial}{\partial X}\left[P_T\frac{\partial a}{\partial X}\right]=\frac{\partial}{\partial X}\left[D_T S\frac{\partial a}{\partial X}\right] \tag{1}$$

could not be fully detected on the basis of the data presented in part 1. To this end, early and long-term transient and steady-state permeation and the corresponding integral sorption data were obtained and treated in the manner described in this study.

Another objective of this investigation was to present a comparison of the concentration dependence of the integral diffusion coefficient $\bar{D}(C)$ obtained by different experimental techniques and methods of data treatment. Also, as shown in part 1, this system exhibits pronounced sorption hysteresis (i.e. for any given penetrant activity the equilibrium concentration in the polymer is always higher along the desorption limb of the isotherm than on the corresponding absorption one). This was qualitatively accounted for in terms of slow molecular relaxation processes. However, a more detailed study of the effect of previous membrane history on the diffusion behaviour was necessary in order to gain further insight on the nature of this phenomenon. To this end, we applied our previously adopted versatile experimental scheme[6,7] (as outlined below) which enables measurement of diffusion rates under both absorption and desorption conditions, not only in sorption kinetics but also in permeation.

Theoretical outline of methods

In accordance with the terminology of part 1[1], the equilibrium activity at $t=0$ throughout a membrane of thickness l is denoted by a_1. The symbols a_0, a_l represent the activities at its two faces, $X=0$ and $X=l$, respectively at all $t>0$ of any of the experiments involved in this work, which are described below:

Integral sorption kinetics. The condition $a_0=a_l$ (with $a_0>a_1$ in absorption and $a_0<a_1$ in desorption) is again applicable. However, in contrast to the differential series, here we always maintained the condition $a_1=0$ and $a_l=0$ in absorption and desorption respectively. Also, the early and late-time diffusion coefficients D_1 and D_2, which can be obtained in terms of the ratio Q_t/Q_∞ (and the other parameters of equations 3 and 4 of part 1[1]) are comparable to the integral values D_1 and D_2 for a series of corresponding differential increments to the same value of $C_0=Sa_0$.

$$Q_t/Q_\infty=4\left[\frac{D_1 t}{\pi l^2}\right]^{1/2} \quad \text{and} \quad ln(1-Q_t/Q_\infty)=ln\left[\frac{8}{\pi^2}\right]-\frac{D_2\pi^2 t}{4l^2}$$

0032-3861/81/081058-06$02.00

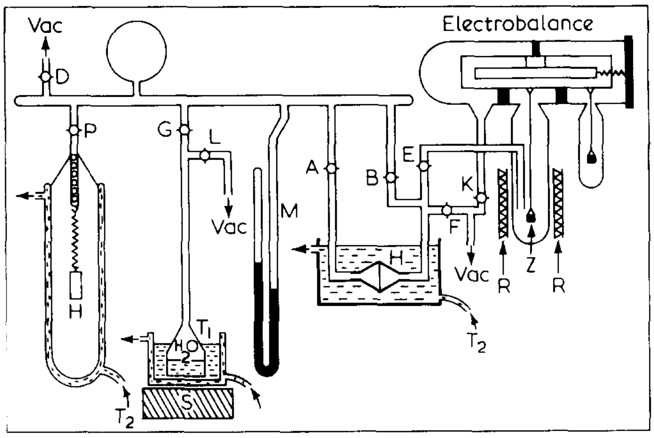

Figure 1 Sorption kinetics and permeation apparatus

Permeation. Here $a_0 > a_l = 0$, so that the penetrant emerging from the latter membrane face per unit of its cross sectional area U (within any t from the start of the experiment) is the measurable quantity, denoted by $Q(l,t)$. Furthermore, we distinguish the following types of permeation[6,7]: (i) absorption permeation with $a_1 = a_i$; (ii) desorption permeation with $a_0 = a_1$.

In either (i) or (ii), as $t \rightarrow \infty$ the flux $q(l,t) = \mathrm{d}Q(l,t)/\mathrm{d}t = P_T(\partial a/\partial X)$ tends to a steady-state value q_s. This follows equation (1) {or, alternatively from the classical formulation of diffusion in which $D = P_T(\partial a/\partial c)$ is substituted in equation (1)} if the steady state condition $\partial c/\partial t = 0$ is applied. Thus, in absorption (desorption) permeation q_s is approached from a lower (higher) value of $q(l,t)$ (*Figure 2*) and the same considerations are applicable for the approach to the steady-state concentration profiles (i.e. C vs. X) within $0 \leqslant X \leqslant l$. The t-axis intercepts of $Q_s^a(l,t)$ and $Q_s^d(l,t)$ in absorption and desorption permeation (which for a system possessing a reversible equilibrium isotherm should be parallel and hence have a common q_s if a_0 (absorption) $= a_1$ (desorption)), are defined as the downstream absorption (positive) and desorption (negative) time lags $L^a(l)$ and $L^d(l)$, respectively[6,7] (*Figure 2*).

The steady-state coefficients P_T and D_e, under the conditions specified above are integral values given by:

$$\bar{P}_T(a,\infty) = \frac{q_s l}{a_0} = \frac{Q_s(l,t)l}{a_0(t-l)} \tag{2}$$

$$\bar{D}_e = \frac{q_s l}{S a_0} = \frac{Q_s(l,t)\cdot l}{(t-L)C_0} \tag{3}$$

Thus $\bar{D}_e$ may be determined only if $C_0 = S a_0$ is known from independent equilibrium data. Alternatively, if the conditions for Fickian diffusion (as discussed in part 1[1]) are fulfilled and if the concentration dependence of $\bar{D}_e$ is known, then $L^d(l)$ or $L^a(l)$ may be directly correlated with steady-state quantities.

To obtain the transient state permeation diffusion coefficients D_3 or D_4, the following early-time solution[8-11] of the diffusion equation

$$\ln[t^{1/2}q(l,t)] = \ln\left[2C_0\left(\frac{D_4}{\pi}\right)\right] - \frac{l^2}{4D_3 t} \tag{4}$$

or its integrated form:

$$\ln[Q(l,t)] = \ln\left[\frac{8C_0}{\sqrt{\pi}}\frac{D_4 t}{l^3}\right]^{3/2} - \frac{l^2}{4D_3 t} \tag{5}$$

may be used.

EXPERIMENTAL

Membranes A and B ($l = 147$ and $95\ \mu$m, respectively) were prepared by the same methods and from the same grade of cellulose acetate as in part 1[1] i.e. by casting solutions of cellulose acetate (39.9% acetyl content) in acetone, on clean glass surfaces. Adjacent pieces of each were used for sorption kinetics and permeation.

The sorption and permeation apparatus (*Figure 1*) contained a vapour generator (which was continuously stirred and thermostatted to the desired temperature T_1 $\pm 0.02^\circ$C) and a closed-end Hg manometer (M) for vapour pressure measurements. Both the jacket surrounding the sorption chamber and the bath in which the permeation cell was immersed, were maintained at $T_2 = 25 \pm 0.05^\circ$C by circulating water from a constant temperature reservoir. Our sorption kinetics technique was identical to the one used in part 1[1]. In the permeation cell either membrane had an active $U = 12.44$ cm^2. The downstream (i.e. beyond $X = l$) compartment of the apparatus contained an aluminium calcium silicate zeolite sample Z, suspended from a Cahn RG–HV electrobalance. The fact that the rate of water sorption in Z was almost instantaneous[12] (compared with that of permeation) enabled us to monitor $Q(l,t)$ in both types of permeation from the net weight gain in Z. Care was taken not to exceed absorption of H_2O in Z beyond the Henry law region[13] so as to trap practically all of the vapour and maintain $a_l = 0$. For this reason, Z was reactivated prior to each experiment by evacuation and heating to 360°C. Also, during extended permeation runs, the electrobalance section was isolated overnight by means of taps E, F (*Figure 1*), during which time the downstream compartment was connected to a liquid N_2 trap in the vacuum line via tap K. Depending on the conditions chosen, a permeation run was begun as follows:

(i) In absorption permeation — The membrane H was evacuated via taps A, B and D with F closed. Prior to a run A, B and D were closed and vapour was admitted to the manifold via G. At $t = 0$, A was opened.

(ii) In desorption permeation—H was first equilibrated at a vapour activity a_1 via A and B with F and E closed. B was then closed and at $t = 0$, F was opened for a time interval t_1, during which the downstream compartment was sufficiently evacuated so as to maintain the boundary condition $a_l = 0$ without saturating Z. At t_1, E was also opened.

Concurrent pairs of permeation and sorption kinetic runs were performed within the same seven concentration integral steps. For the series of desorption permeation and kinetics along the upper limb of the isotherm, prior to each run the membrane was initially equilibrated at $a = 1$ (saturation) and then desorbed to a_1.

RESULTS AND DISCUSSION

Steady-state permeation and time lag analysis

In all permeation runs (especially those at higher C_0), the approach to the true steady state flux $q_s(a,\infty)$ was

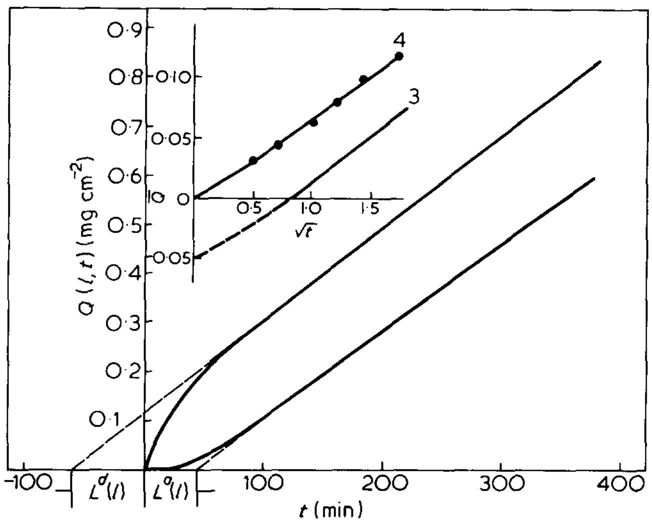

Figure 2 Permeation through membrane A with $a_0 = 0.194$. Curves: 1, absorption; 2, desorption; 3, early time desorption (Q/lC_0 vs. $\sqrt{t}$); 4, early time desorption kinetics ($1/2\ Q_t/Q_\infty$ vs. $\sqrt{t}$)

extremely slow, whether this was attained from a higher or a lower transient value in desorption or absorption permeation, respectively. It was found necessary to prolong most runs (to a greater extent those on the thicker membrane A) for as long as three days before an apparently constant value of q_s could be recorded.

In desorption permeation, although t_1, i.e. the time elapsed between $t=0$ and discontinuation of downstream side evacuation (see Experimental), was only 15 s, yet in view of the high initial permeation rates in these cases (*Figure 2*, curve 2) it is still sufficient to cause a significant amount of penetrant to be lost from that compartment of the apparatus. This had no effect on q_s, but introduced a source of negative error (though not as high as in other cases[7] due to S-shape desorption) in the measured $L^d_s(l)$. To correct for this, we fitted the early-time permeation curve to that of the corresponding integral desorption kinetic data within the same concentration interval. {Note that, as we have previously discussed[7], for a homogeneous diffusion barrier at sufficiently low t, $\bar{Q}(t) = Q(l,t)/lC_0 = 1/2Q_t/Q_\infty$}. The method is illustrated in the inset of *Figure 2*.

From a least square fitting of $Q_s(l,t)$ vs. t of the first day's portion of a permeation run (i.e. from a pseudo-steady state), we obtained $L^a_s(l)$ or $L^d_s(l)$, depending on the type of experiment concerned (equation 3). The error involved in this practice could not be avoided in the apparatus of *Figure 1* without exceeding the Henry-law sorption region of the zeolite (thus causing incomplete trapping of vapour in Z, as well as violation of the boundary conditions). However, we note that there is no error involved in the measurement of $Q(l,t)$ or t, but only of the slope q_s. Hence (according to equation 3), the actual $L^a_s(l)$ and $L^d_s(l)$ should be more positive and negative, respectively, and as a result the absolute values of these quantities in *Table 1* represent minimum ones. However, $\bar{D}_e$ was obtained from the limiting q_s measured in the last day's portion of a run, according to equation 3 with C_0 expressed in polymer frame of reference units (g cm^{-3} of dry polymer). The concentration dependence of $\bar{D}_e$ was then fitted to a polynomial of the form:

$$\bar{D}_e(C_0) = \bar{D}_e(0)\{1 + k_1 C_0 + k_2 C_0^2\} \qquad (6)$$

These data (*Figure 3*) show that $\bar{D}_e$ is concentration increasing in all cases and that for either membrane along the lower limb of the isotherm, the desorption permeation $\bar{D}_e$ values are higher than the corresponding absorption permeation ones (compare curves 1A vs. 2A and 1B vs. 2B, *Figure 3*). A better $\bar{D}_e$ vs. C_0 agreement is to be observed (especially at lower concentrations) when desorption permeation results are compared between the two limbs of the equilibrium isotherm.

The corresponding Fickian time lags L^a_s and L^d_s were, in turn, estimated by means of the following expressions[9]:

$$L^a_s = \int_0^l C D_e(C)\left[\int_C^{C_0} D_e(C)\mathrm{d}C\right]\mathrm{d}C \Big/ q_s^3 l \qquad (7)$$

$$L^d_s = L^a_s(l) - lC_0/2q_s \qquad (8)$$

Also, since by definition, $D_e(C)$ of equation 6 is related by[1,8]:

$$\bar{D}_e(C_0) = \frac{1}{C_0}\int_0^{C_0} D_e(C_0)\mathrm{d}C \qquad (9)$$

our empirical equation 6 gave the following expression which was analytically integrated within equation 7,

$$D_e(C_0) = D_e(0)\{1 + 2k_1 C_0 + 2k_2 C_0^2\} \qquad (10)$$

Thus, in addition to $L^a(l)$, the absorption–desorption difference δL and the normalized non-Fickian increments

Table 1 Time lag analysis (membrane A)

a_0	C_0 (g cm^{-3})	$L^a(l)$ (min)	δL (min)	L^a_T/L^a_S	$\delta L_T/\delta L_S$
0.194	0.0230	42	102	0.4	0.2
0.424	0.0497	35	83	0.2	0
0.554	0.0688	47	91	0.8	0.2
0.657	0.0863	46	79	0.7	0.1
0.749	0.1062	46	91	1.1	0.5
0.837	0.1316	57	86	2.3	0.8
0.917	0.1618	47	86	1.9	1.2

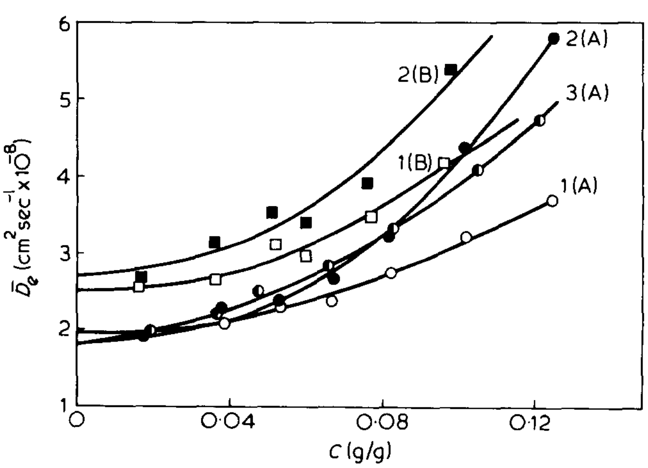

Figure 3 Concentration dependence of $\bar{D}_e$ from permeation through membranes A and B. Absorption (1) and desorption along lower and upper limbs of hysteresis (2 and 3)

Table 2 Transient-state permeation diffusion coefficients (membrane A) $cm^2\ s^{-1} \times 10^{-8}$

C_0 (g cm^{-3})	Equation 4		Equation 5	
	D_4	D_3	D_4	D_3
0.0230	3.72	1.39	1.60	1.21
0.0497	2.65	1.61	1.92	1.19
0.0688	1.79	2.06	1.19	1.91
0.0863	2.16	2.13	1.68	1.29
0.1062	2.66	1.87	1.43	1.69
0.1316	5.61	1.68	1.74	1.60
0.1618	8.27	1.73	1.74	1.76

L_T/L_s and $\delta L/\delta L_s$, defined as[6]

$$\delta L = L^a - L^d$$
$$L^a_T/L_s = (L^a - L^a_s)/L^a_s \qquad (11)$$
$$\delta L_T/\delta L_s = (\delta L - \delta L_s)/\delta L_s$$

are also included in *Table 1*.

In the line of our previous arguments we can verify the algebraic sign of these non-Fickian increments in *Table 1*, also considering that there is no error involved in the estimation of L^a_s and δL_s, since they were obtained from the true steady-state flux $q_s(l,\infty)$ in terms of equations 7, 8 and 11. Hence, though the uncertainty in the magnitude of these figures deprives us of a quantitative treatment, yet we can still draw some valuable conclusions with regard to the nature of our diffusion system. As previously[2,5,6], we formulate that the transient state coefficient $P_T(a,t)$ is approaching its steady-state limit $P_T(a,\infty)$ in a way similar to that used for the approach to equilibrium of $C(a,t)$ in part 1[1], i.e.

$$\frac{\partial P_T}{\partial t} = \frac{\partial P_T(a,t)}{\partial a}\frac{\partial a}{\partial t} + \beta\left[P_T(a,\infty) - P_T(a,t)\right] \qquad (12)$$

where β is a rate parameter expressing a spectrum of relaxation frequencies. Analysis of equation 1 along with equation 12 yielded the following expression for L^a_T

$$L^a_T = \int_0^t \mathrm{d}t \int_{a_l}^{a_0} [P_T(a,\infty) - P_T(a,t)]\mathrm{d}a \Bigg/ \int_{a_l}^{a_0} P_T(a,\infty)\mathrm{d}a \qquad (13)$$

which has already been satisfactorily applied to interpret literature time lag data[5]. An identical expression may also be given for L^d_T, keeping also in mind that the sign of $P_T(a,\infty) - P_T(a,t)$ in equation 13 is reversed in the case of desorption. Hence, if $P_T(a,t)$ increases with t during absorption permeation, then L^a_T and L^d_T should be positive and negative, respectively, also causing (according to equation 11) δL_T to be positive. This is exactly the case L^a_T and δL_T in the data of *Table 1*. As the magnitude of these non-Fickian increments seems to increase with C_0 further confirms the idea of a time increasing $P_T(a,t)$, which is also consistent with the observation that $q_s(a,\infty)$ is approached at an appreciably slow rate

Transient-state permeation

Treatment of our absorption permeation data was carried further by graphical determination of $q(l,t)$ at several times in the transient state within the interval $0 \leqslant t \leqslant 100$ min. These values were in turn used to construct plots of the left-hand-side terms of equation 4 vs. $1/t$, which for the thicker membrane, A, fell on straight lines, while for membrane B (whose appreciably faster permeation rates caused increased uncertainty in determination of q) a significant scatter of points was shown. *Table 2* gives D_3 and D_4 obtained by the slope and ordinate-intercept of these plots, respectively. These data show that D_3 fluctuates only between 1.4–2.1 $cm^2\ s^{-1} \times 10^{-8}$ (i.e. it does not range beyond the limits of experimental and graphical accuracy) and averages to 1.8×10^{-8} $cm^2\ s^{-1}$, which is the value of our empirical $\bar{D}_e(0) = D_e(0)$ of equation 10 (as shown also in *Figure 3*, curve 1A at $C_0 = 0$). This, however, is not the case with D_4 whose values seem to depart considerably from those of D_3. Similar trends have also been reported by Meares[14], who has used equation 4 for a polymer–penetrant system close to T_g. Meares has pointed out that the accuracy in obtaining D_4 from the intercept of equation 4 is limited, since that term also contains Sa_0 which is concentration dependent. In our case there is additional justification to this line of reasoning, bearing in mind that (as already shown in part 1) S is also strongly time dependent. However, *Table 2* shows that when the integral form of equation 4 (i.e. equation 5) was used, closer agreement between D_3 and D_4 was achieved. An explanation of this follows by comparison of equations 4 and 5, as in the latter the relative weight of Sa_0 is diminished. The fact that disagreement between D_3 and D_4 increases with increasing C_0 (*Table 2*, results of equation 4) is also consistent with these arguments.

Integral sorption kinetics

The small-time kinetic curves for integral absorption runs were definitely S-shaped on a $\sqrt{t}$ scale and this

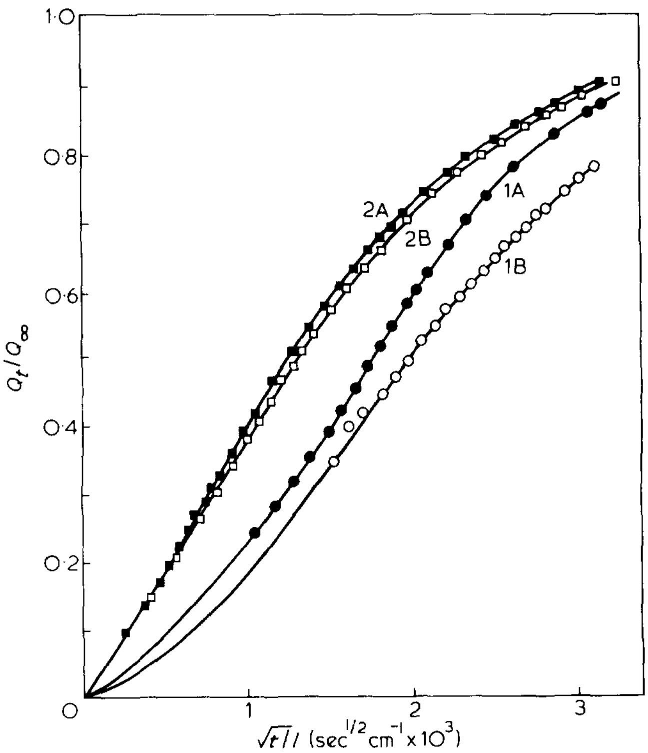

Figure 4 Integral sorption kinetics on membranes A and B, with a_0 = 0.838. Curves: 1, absorption; 2, desorption

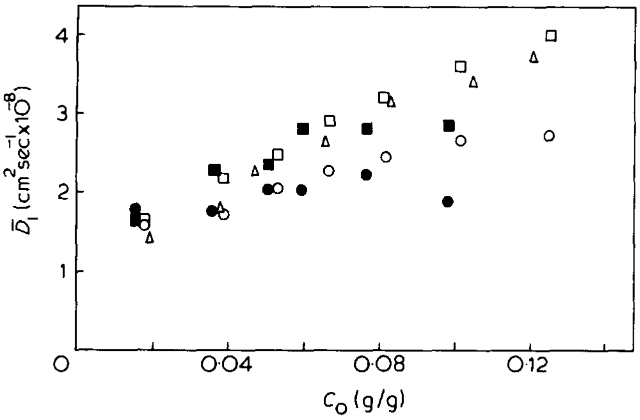

Figure 5 Concentration dependence of $\bar{D}_1$ from sorption kinetics: ○, ● absorption; □, ■, △ desorption; ○, □, △, membrane A; ●, ■ membrane B; △, upper limb and all other points along lower limb of hysteresis

feature became more intense at higher C_0 (*Figure 4*). However, contrary to the differential absorption series of part 1, even at the highest C_0(0.125 g/g) applied, there was no indication of two-stage kinetics.

Since the measurements here concerned only two membranes, it was not possible to apply our extrapolation procedure to $l \rightarrow \infty$ (see part 1)[1] with certainty in order to separate diffusion from other rate-controlling processes. Instead, we obtained apparent $\bar{D}_1$ from the slope of the initial portion of every Q_t/Q_∞ vs. $\sqrt{t}/l$ curve (which was a method also applied in part 1). Nevertheless, the increase in initial slope (of Q_t/Q_∞ vs. t/l) with increase in l, which has been shown to characterize the differential sorption series[1], also occurred in the integral runs of this study. This trend is apparent in *Figure 4* in absorption and to a lesser extent in desorption for one concentration interval. However, it also persists at all concentrations, as illustrated in the data of *Figure 5*, i.e. the estimated $\bar{D}_1$ values (in either absorption or desorption) are at most concentrations higher for the thicker membrane A. The apparent coincidence of $\bar{D}_1$ in the two membranes at low C_0 can be attributed to the significantly smaller variation of l used in this study in comparison with those of part 1.

The data of *Figure 5* also show reasonable agreement with those of permeation (*Figure 3*) in that $\bar{D}_1$ increases with C_0 in both membranes in desorption as well as in absorption (the latter to a lesser degree on membrane B, see below. For a given membrane $\bar{D}_1$ from desorption is, at all C_0, higher than that from absorption consistent with our steady-state permeation results. The coincidence of $\bar{D}_1$ in desorption (throughout the entire concentration range of our data) along the two limbs of the equilibrium isotherm, constitutes a remarkable duplication of the trends in permeation. These observations imply that in this system a kinetic hysteresis also seems to exist (i.e. when $\bar{D}_1$ from absorption as well as from desorption is comparatively plotted against a) whose shape is similar to that of the equilibrium sorption isotherm. This trend is also in conformity with the evidence presented in part 1 that along the desorption limb of the isotherm, the polymer possesses a more open structure and, as a result, initial state desorption proceeds at a faster rate than the corresponding absorption one.

In contrast to the differential sorption series, a distinguishing trait of the transient-state integral desorption kinetics is that they exhibit a less marked initial S-shape, especially at higher C_0 (e.g. *Figure 4*, curves 2A, 2B). The possibility of non isothermal diffusion as a result of membrane cooling[1,15] (due to appreciable heat of sorption), as well as the effect of transverse swelling stresses[16,17] were both not considered likely as determining factors in the case of our differential sorption series. In the present study, which involves considerably larger concentration intervals it is possible that these may play a more important role. However, we are led to believe that the effect of molecular relaxations still predominates, since plots of Q_t (in weight of penetrant per unit membrane surface) vs. $\sqrt{t}$ did not possess the characteristic features of the differential stress model[16-18], as at all times the thicker membrane absorbed more penetrant than the thinner one. Further weight to the effect of molecular relaxations is gained by the fact that late-time desorption rate curves {i.e. ln $(1 - Q_t/Q_\infty)$ vs. t, according to equation 4 of part 1} exhibited intense curvature, which (as in part 1) hindered calculation of $\bar{D}_2$ (in fact to a greater extent than the corresponding absorption ones). This non-Fickian characteristic cannot be attributed to heat effects, which are expected to prevail during the early stages of sorption. However, the long term change in P_T with t, demonstrated to occur in permeation, can reasonably account for the shape of these late-time sorption kinetic curves.

SUMMARY AND CONCLUSIONS

The slow molecular relaxations of this system documented in part 1[1], have been definitely confirmed in the results of this study. Our steady-state and time lag permeation data also provide evidence that P_T slowly increases (decreases) with t in absorption (desorption), thus resembling the trends in S. Consequently, the mobility D_T of penetrant does not seem to be sufficiently decreasing as a result of its partial immobilization in clusters. We are thus led to the conclusion that the net effect of these molecular relaxations is that the relatively large cavities in the polymer, which are necessary to accommodate clusters, are being formed independently of the smaller ones which receive monomeric penetrant and not at their expense (i.e. contrary to the case of ethyl cellulose[19] discussed in part 1[1] and previously[5]). It is also likely that the mobility of monomeric species itself may actually be enhanced due to polymer plastisization, to an extent that causes the overall mobility $D_T = D_T(m)S(m)/S$ to increase slightly with t. In this respect, we note that contradictory conclusions[2] were to be drawn for cellulose acetate–water vapour on the basis of previously published experimental evidence[20].

Our indirect evidence (in part 1) that D increases with C_0 in both branches of the equilibrium isotherm has also been confirmed in this study, especially on the basis of our long-term permeation data, which enabled us to clearly separate diffusion from rate-controlling molecular relaxations. Our $D_e(C_0)$ relationship derived from these results (in terms of the empirical constants $2k_1$, $2k_2$ of equation 9) extrapolates to approximately 1×10^{-7} cm^2 s^{-1} at saturated vapour concentration. It is interesting to note that this value is of the same order of magnitude as that reported for liquid water transport in a similar grade of cellulose acetate, as determined by selfdiffusion with tritium isotope methods[21,22].

ACKNOWLEDGEMENTS

This work was sponsored by the Hellenic Atomic Energy Commission. The interest and many helpful suggestions of Dr J. H. Petropoulos are appreciated. Thanks are also due to Mr D. Skordilis for laboratory assistance.

REFERENCES

1 Roussis, P. P. *Polymer* 1980, in press
2 Petropoulos, J. H. and Roussis, P. P. 'Permeability of Plastic Films and Coatings to Gases, Vapors and Liquids' (Ed. H. B. Hopfenberg), Plenum, New York, 1974, pp 219–232
3 Barrie, J. A. 'Diffusion in Polymers' (Eds. J. Crank and G. S. Park), Academic Press, New York, 1968, Ch 8, pp 259–308
4 Petropoulos, J. H. and Roussis, P. P. 'Organic Solid State Chemistry' (Ed. G. Adler), Gordon and Breach, London, 1969, Ch 19, pp 343–357
5 Petropoulos, J. H. and Roussis, P. P. *J. Polym. Sci. (C)* 1969, **28**, 343
6 Petropoulos, J. H. and Roussis, P. P. *J. Chem. Phys.* 1967, **47**, 1491
7 Roussis, P. P. and Petropoulos, J. H. *J. Chem. Soc. Faraday II* 1976, **72**, 737
8 Crank, J. 'Mathematics of Diffusion', Claredon, London, 1975, Ch 4, pp 44–69
9 Frisch, H. L. *J. Phys. Chem.* 1957, **61**, 93
10 Rogers, W. A., Buritz, R. S. and Alpert, D. J. *Appl Phys.* 1954, **25**, 868
11 Felder, R. M. *J. Membrane Sci.* 1978, **3**, 15
12 Timofeev, D. T. and Kabanova, O. N. *Izv. Acad. Nauk. S.S.S.R., Otd. Khim. Nauk* 1961, **9**, 1539
13 Breck, D. W., Eversole, W. G., Milton, R. M., Reed, T. B. and Thomas, T. L. *J. Am. Chem. Soc.* 1956, **78**, 5963
14 Meares, P. *J. Appl. Polym. Sci.* 1965, **9**, 917
15 Armstrong, A. A., Wellons, J. D. and Stannett, V. *Makromol. Chem.* 1966, **95**, 78
16 Crank, J. *J. Polym. Sci.* 1953, **11**, 151
17 Petropoulos, J. H. and Roussis, P. P. *J. Membrane Sci.* 1978, **3**, 343
18 Blackadder, D. A. and Keniry, J. S. *J. Appl. Polym. Sci.* 1974, **18**, 699
19 Wellons, J. D. and Stannett, V. *J. Polym. Sci. (A-1)* 1966, **4**, 593
20 Wellons, J. D., Williams, J. L. and Stannett, V. *J. Polym. Sci. (A-1)* 1967, **5**, 1341
21 Thau, G., Block, R. and Kedem, O. *Desalination* 1966, **1**, 129
22 Yasuda, H., Lamaze, C. E. and Peterlin, A. *J. Polym. Sci. (A-2)* 1971, **9**, 1117